Current Optics and Photonics
Vol. 1, No. 6, December 2017, pp. 649-654
ISSN: 2508-7266(Print) / ISSN: 2508-7274(Online)
DOI: https://doi.org/10.3807/COPP.2017.1.6.649

Fully Analytic Approach to Evaluate Laser-induced Thermal Effects

Myungsoo Kim[1], Gyeong-Pil Kwon[2], and Jinho Lee[3]*

[1]*Department of Mechanical Design Engineering, Youngsan University, Yangsan 50510, Korea*
[2]*Department of Science Education, Gyeongin National University of Education, Incheon 21044, Korea*
[3]*The Research Institute of Natural Science and Department of Physics Education, Gyeongsang National University, Jinju 52828, Korea*

(Received August 22, 2017 : revised September 21, 2017 : accepted September 27, 2017)

In this communication, we present an expression to determine thermal lensing in isotropic materials. The heat equation is analytically solved when a Gaussian spatial laser beam profile is introduced to a cylindrical geometry of optics using a complete set of Bessel functions. This expression permits explicit calculation of variation of focal length induced by thermal lensing and allows thermal effects for various material parameters on the optics. We applied our model to a high absorption material (Ti:sapphire) and also transparent material (thallium garnet or TGG) and found that the thermal lensing can be reduced more than 4 times by adjusting the laser beam waist and optics dimensions. Our analysis is completely general and applicable to any optical system.

Keywords : High power laser, Thermal lensing
OCIS codes : (350.6830) Thermal lensing; (120.6810) Thermal effects; (140.3295) Laser beam characterization

I. INTRODUCTION

High-power lasers have revolutionized highly nonlinear processing in atomic, molecular, plasma and solid state physics making it possible to access previously unexplored states of materials [1]. However, increasing laser power while maintaining laser beam quality requires careful consideration of beam distortion caused by thermal effects [1-3]. In general, high power laser generates mechanical stress in all optical elements, because the hotter inside area is constrained from expansion by the cooler outer zone [4]. The stresses in the optical elements caused by a temperature distribution $T(r)$ generate thermal strains in the rod, which, in turn, produce refractive index variation via a photoelastic effect called thermal lensing [4].

Several studies have been carried out on thermal lensing in the field of high power laser technologies [5-7] and also in the laser interferometer gravitational-wave observatory (LIGO) [1-3, 8, 9], because high beam quality is crucial to measure weak gravitational wave signals. To address the issue of beam distortion from thermal lensing, a number of techniques have been suggested that compensate for thermal aberrations, using compensating materials with opposite temperature derivatives of the refractive index [8, 10], CO_2 laser heating and electrical heating of the optical elements [3, 11, 12], tunable liquid crystals [13] and deformable mirrors [14]. In response to the rising demands for new technologies, the thermal lensing phenomenon itself can be employed in new kinds of measuring equipment such as thermal lens microscope [15, 16] and confocal thermal lens microscope [17].

Since Koechner pioneered the field of laser engineering (see [4] and references herein), a number of analytic solutions for thermal lensing have been presented. For example, Koechner [18], Farrukh [19], Innocenzi [20], Cousins [21], and Schmid *et al*. [22] have derived the solution for a super-Gaussian laser beam and the general solution for an infinite cylinder is given in [23]. However, to our knowledge, none of these analyses has solved the exact analytic thermal expression in a finite cylindrical geometry for Gaussian spatial profile with convection boundary conditions.

*Corresponding author: lee.phys.edu@gnu.ac.kr, ORCID 0000-0002-9452-6630
Color versions of one or more of the figures in this paper are available online.

In this paper, we present the analytic temperature distribution in the cylindrical geometry of the optics induced by the Gaussian spatial beam profile of the input laser and derive a simple focal length expression to examine the thermal effects depending on material parameters such as input laser beam waist, laser power, and radial and longitudinal dimensions of the optics. Our analysis is completely general and applicable to all optic systems.

II. THEORY

We started our analysis with the classical steady-state heat transfer equation with the source term $S(r,z)$ corresponding to the Gaussian spatial profile:

$$-\kappa\nabla^2 T = S(r,z) \tag{1}$$

where κ is the thermal conductivity. For this study, we consider that the physical properties of the material (thermal conductivity, absorption coefficient, etc.) stay constant over the range of temperatures involved in the heat equation and the heat transport within the material is isotropic [24].

As illustrated in Fig. 1, when the Gaussian laser beam travels through the cylindrical geometry of the laser rod with radius $a(0 \le r \le a)$ and length $l(0 \le z \le l)$, $S(r,z)$ in Eq. (1) could be represented as:

$$S(r,z) = -\frac{2\alpha P}{\pi\omega^2} e^{-2\frac{r^2}{\omega^2}} e^{-\alpha z} \tag{2}$$

where α is the absorption coefficient, P is the power of the input laser and ω is the Gaussian beam waist.

For the boundary conditions, we assume that the laser crystal is in thermal contact with a liquid-cooled holder to maintain a constant temperature at the cylindrical surface.

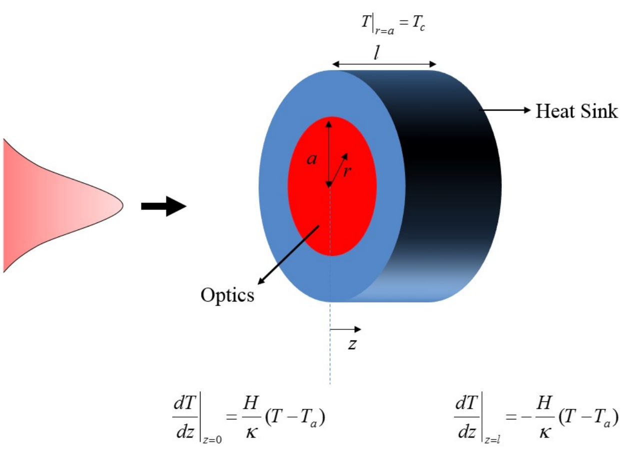

FIG. 1. When the Gaussian spatial profile of the laser beam traverses the optics, thermal lensing occurs within the optical element with radius $a(0 \le r \le a)$ and length $l(0 \le z \le l)$.

The cooling at both ends is proportional to the temperature rise T of the surface above the ambient temperature [24]

$$\kappa\vec{n} \bullet \nabla T + H_L T = 0 \tag{3}$$

where H_L refers to the heat transfer coefficient for the appropriate surface, and $\vec{n}$ is the direction of the outward surface normal. In general, H_L can be presented as the sum of two contributions from radiative cooling and active cooling [25]

$$H_L = H_{radiative} + H_{active\ cooling} \tag{4}$$

with $H_{radiative} = 4\varepsilon\sigma T_a^3 \approx 6.5W/(m^2K)$ where $\varepsilon \approx 1$, $\sigma = 5.67 \times 10^{-8} W/(m^2K^4)$ and $T_a \approx 300K$ are the surface emissivity, Stefan-Boltzmann constant, and the ambient temperature measured in Kelvin [19], respectively and $H_{active\ cooling} \approx 10W/(m^2K)$ according to Ref. [25]. As described in our previous works using an orthogonal complete set of Bessel functions (the detailed descriptions are presented in [24] and [26]), the general solution of Eq. (1) can be expressed in terms of the Bessel functions $J_0\left(k_n \frac{r}{a}\right)$ with k_n, roots of $J_0(k_n) = 0$.

$$T = \sum_{n=1}^{\infty} A_n J_0\left(k_n \frac{r}{a}\right) f_n(z) + T_a \tag{5}$$

where T_a is the initial temperature of the optics before the laser arrives and is the same as the ambient temperature (in this study, the coolant temperature is equal to the ambient temperature T_a). After substituting Eq. (5) into Eq. (1) and using the orthogonality of the Bessel function [26] and the identity of the Bessel differential equation

$$\int_0^a r J_0(k_n \frac{r}{a}) J_0(k_m \frac{r}{a}) dr = \frac{a^2}{2} J_1(k_n)^2 \delta_{nm} = \frac{a^2}{2} J_0(k_n)'^2 \delta_{nm} \tag{6}$$

$$\frac{1}{r}\frac{d}{dr}[r\frac{dJ_0(k_n \frac{r}{a})}{dr}] + \frac{k_n^2}{a^2} J_0(k_n \frac{r}{a}) = 0 \tag{7}$$

we find the coefficient A_n

$$A_n = -\frac{2\alpha P}{\pi\kappa\omega^2} \frac{\int_{r=0}^{a} e^{-2\frac{r^2}{\omega^2}} J_0\left(k_n \frac{r}{a}\right) r dr}{\frac{a^2}{2} J_1(k_n)^2}. \tag{8}$$

Thus, the z-dependent function f_n satisfies the following equation

$$-\frac{k_n^2}{a^2} f_n(z) + \frac{\partial^2}{\partial z^2} f_n(z) = e^{-\alpha z} \tag{9}$$

and the boundary condition of Eq. (3) at the two ends of the laser rod are

$$\left.\frac{\partial f_n(z)}{\partial z}\right|_{z=0} = \frac{H_L}{\kappa} f_n(z)\Big|_{z=0} \tag{10}$$

$$\left.\frac{\partial f_n(z)}{\partial z}\right|_{z=l} = -\frac{H_L}{\kappa} f_n(z)\Big|_{z=l} \tag{11}$$

The solution of Eq. (9) with the boundary conditions (10) and (11) will result in

$$\begin{aligned} f_n(z) = & \frac{1}{\alpha^2 - \frac{k_n^2}{a^2}} \frac{a}{k_n} \frac{1}{(1-\frac{H_L}{\kappa}\frac{a}{k_n})^2 e^{-\frac{k_n}{a}l} - (1+\frac{H_L}{\kappa}\frac{a}{k_n})^2 e^{\frac{k_n}{a}l}} \\ & \times [e^{-\frac{k_n}{a}l} e^{\frac{k_n}{a}z} (\alpha + \frac{H_L}{\kappa})(1-\frac{H_L}{\kappa}\frac{a}{k_n}) \\ & - e^{-\alpha l} e^{\frac{k_n}{a}z} (\alpha - \frac{H_L}{\kappa})(1+\frac{H_L}{\kappa}\frac{a}{k_n}) \\ & + e^{\frac{k_n}{a}l} e^{-\frac{k_n}{a}z} (\alpha + \frac{H_L}{\kappa})(1+\frac{H_L}{\kappa}\frac{a}{k_n}) \\ & - e^{-\alpha l} e^{-\frac{k_n}{a}z} (\alpha - \frac{H_L}{\kappa})(1-\frac{H_L}{\kappa}\frac{a}{k_n})] \\ & + \frac{1}{\alpha^2 - \frac{k_n^2}{a^2}} e^{-\alpha z} \end{aligned} \tag{12}$$

As a result, analytic temperature profiles induced by the Gaussian laser can be represented by substituting A_n (Eq. 8) and f_n (Eq. 12) into Eq. (5). Figure 2(a) shows the temperature distribution of a Ti:sapphire laser rod when a 532 *nm* Gaussian beam is introduced to the one end of the rod. The maximum temperature rise is approximately 23 *K* when the laser power is 10 *W*, as shown in the figure. Because Eq. (5), (8), and (12) are also applicable to highly transmissive optics such as thallium garnet (TGG), we also plot the temperature profile of TGG in Figure 2(b) with a 10 *kW* input laser.

Because in Eq. (12), the coefficient H_L always comes together with $1 \pm \frac{H_L}{\kappa}\frac{a}{k_n}$ or $\alpha \pm \frac{H_L}{\kappa}$, the expression of $f_n(z)$ can be further simplified depending on the material properties of the optics. For example, in the case of lasing materials such as Ti:sapphire having a high thermal conductivity and optical absorption coefficient with a moderate optic size (~10 *mm* radius), we approximate $\frac{\kappa k_n}{a} \approx 7920$ and $\alpha\kappa \approx 8250 >> H_L \approx 16.5W/m^2K$. Thus, it is a good approximation to set $1 \pm \frac{H_L}{\kappa}\frac{a}{k_n} = 1$ and $\alpha \pm \frac{H_L}{\kappa} = \alpha$. A similar approximation can be applied to Nd:YAG ($\kappa = 11.2W/(mK)$ and $\alpha = 10 \times 10^2/m$).

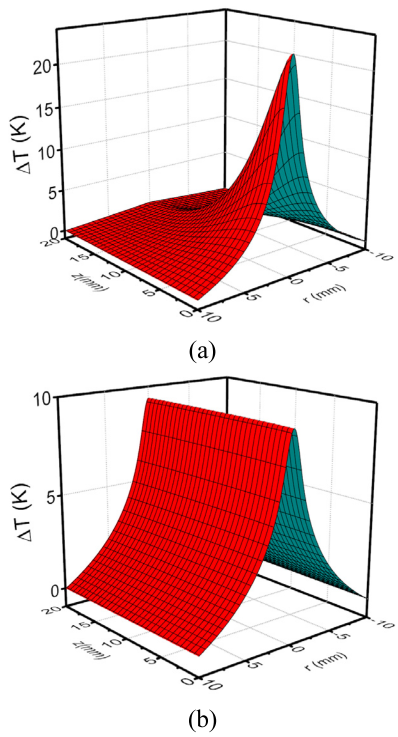

FIG. 2. Temperature distribution in (a) a Ti:sapphire laser rod and (b) a TGG crystal. The radial and the longitudinal lengths of the crystal are 10 *mm* and 20 *mm*, respectively, in both cases. Parameters for the Ti:sapphire laser: 532 *nm* laser power of 10 *W*, beam waist of 1 *mm* and absorption coefficient (α), thermal conductivity (κ), and the surface heat transfer coefficient (H_L) of 2.5 × 10^2 /*m*, 33 *W*/(*mK*) and 16.5 *W*/(m^2K), respectively. Parameters for the TGG: 1064 *nm* laser power of 1 *KW*, beam waist of 1 *mm* with $\alpha = 0.15/m$, $\kappa = 7.4W/(mK)$, and H_L =16.5 *W*/(m^2K).

For the case of transparent materials like thallium garnet (TGG) having a relatively low thermal conductivity and absorption coefficient ($\kappa = 7.4W/(mK)$ and $\alpha = 1.27 \times 10^{-2}/m$), with a moderate optic size, we could approximate $1 \pm \frac{H_L}{\kappa}\frac{a}{k_n} \approx 1$ and $\alpha \pm \frac{H_L}{\kappa} \approx \pm\frac{H_L}{\kappa}$.

Because refractive indices vary with temperature, the refractive index variation in the optics under various temperature distributions could affect the optical path length during the passage of the beam through the laser material. The different degree of physical expansion of the laser material due to a different temperature distribution in the material inside will also result in changes in the optical path length. Accordingly, we need to take into account both contributions to investigate the thermal load in the material.

Optical path length difference, $\Delta l(r)$, resulting from these two effects can be expressed as

$$\Delta l(r) = \gamma \int_{z=0}^{z=L} \Delta T(r,z)dz \tag{13}$$

where $\gamma \equiv \frac{dn}{dT} + \alpha_{\text{expansion}}(n-1)$. n, $\Delta T(r,z)$, $\frac{dT}{dn}$, and $\alpha_{\text{expansion}}$ are the refractive index, temperature change at position r and z, temperature derivative of refractive index, and the thermal expansion coefficient, respectively. Integrating Eq. (13) with the given temperature profile of Eq. (5), the optical path length will be

$$\Delta l(r) = -\sum_{n=1}^{\infty} \frac{\gamma\alpha P}{\pi\kappa} \frac{e^{-\frac{\omega^2 k_n^2}{8a^2}}}{a^2 J_1(k_n)^2} J_0\left(k_n \frac{r}{a}\right) l_z \tag{14}$$

where we used the relation

$$\int_{r=0}^{a} e^{-2\frac{r^2}{\omega^2}} J_0\left(k_n \frac{r}{a}\right) r dr \approx \int_{r=0}^{\infty} e^{-2\frac{r^2}{\omega^2}} J_0\left(k_n \frac{r}{a}\right) r dr = \frac{\omega^2}{4} e^{-\frac{\omega^2 k_n^2}{8a^2}}$$

because in general $a > \omega$ [26] and l_z is

$$\begin{aligned} l_z \equiv \int_{z=0}^{z=l} f_n dz = & \frac{1}{\alpha^2 - \frac{k_n^2}{a^2}} \frac{a^2}{k_n^2} \frac{1}{(1-\frac{H_L}{\kappa}\frac{a}{k_n})^2 e^{-\frac{k_n l}{a}} - (1+\frac{H_L}{\kappa}\frac{a}{k_n})^2 e^{\frac{k_n l}{a}}} \\ & \times[-(e^{-\frac{k_n l}{a}} - 1)(\alpha + \frac{H_L}{\kappa})(1 - \frac{H_L}{\kappa}\frac{a}{k_n}) \\ & + e^{-\alpha l}(1 - e^{\frac{k_n l}{a}})(\alpha - \frac{H_L}{\kappa})(1 + \frac{H_L}{\kappa}\frac{a}{k_n}) \\ & + (e^{\frac{k_n l}{a}} - 1)(\alpha + \frac{H_L}{\kappa})(1 + \frac{H_L}{\kappa}\frac{a}{k_n}) \\ & - e^{-\alpha l}(1 - e^{-\frac{k_n l}{a}})(\alpha - \frac{H_L}{\kappa})(1 - \frac{H_L}{\kappa}\frac{a}{k_n})] \\ & + \frac{1}{\alpha} \frac{1}{\alpha^2 - \frac{k_n^2}{a^2}}(1 - e^{-\alpha l}) \end{aligned} \tag{15}$$

Using the fact that a zero-order Bessel function around $r = 0$ is $J_0(k_n \frac{r}{a}) \approx 1 - (\frac{k_n r}{2a})^2$ when $k_n \frac{r}{a} << 1$ and a spherical lens of curvature from the quadratic form of the optical path length difference is $\Delta l \approx -\frac{r^2}{2R}$, we could get $f = \frac{R}{n-1}$ and so the effective focal length induced by the input laser will be

$$f = -\frac{1}{2(\frac{dn}{dT}(n-1) + \alpha_{thermal}(n-1)^2)\sum_{n=1}^{\infty} \frac{\alpha P}{\pi\kappa} \frac{l_z e^{-\frac{\omega^2 k_n^2}{8a^2}}}{a^2 J_1(k_n)^2} \left(\frac{k_n^2}{4a^2}\right)} \tag{16}$$

For the lasing materials such as Ti:sapphire or Nd:YAG, l_z of Eq. (16) can be simplified as

$$l_z \approx -\frac{a^2(1-e^{-\alpha l})}{\alpha k_n^2} \tag{17}$$

with $1 \pm \frac{H_L}{\kappa}\frac{a}{k_n} = 1$ and $\alpha \pm \frac{H_L}{\kappa} = \alpha$ as mentioned before. For transparent optics such as TGG and fused silica, with the assumption of $1 \pm \frac{H_L}{\kappa}\frac{a}{k_n} \approx 1$ and $\alpha \pm \frac{H_L}{\kappa} \approx \pm\frac{H_L}{\kappa}$, l_z can be approximated as

$$l_z \approx \frac{1}{\alpha^2 - \frac{k_n^2}{a^2}}[-\frac{a^2}{k_n^2}\frac{H_L}{\kappa}(1 + e^{-\alpha l}) + \frac{1}{\alpha}(1 - e^{-\alpha l})] \tag{18}$$

III. DISCUSSION

Because the focal length expression of Eq. (16) originates from the laser-induced thermal load on the material, we could use this to estimate the thermal effects. When there is no input laser ($P = 0$), the focal length induced by the laser should be infinite as seen in Eq. (16) and, in general, the focal length induced by the laser is inversely proportional to the input laser power.

Because the temperature profile follows the input spatial profile of the laser beam, a broader temperature distribution could be generated from a larger beam waist of the laser and, consequently, we can get a larger focal length (or less thermal effect) from the thermal load. As shown in Figure 3(a), although the geometry of optics and input laser power are constant, we could vary the focal length of the Ti:sapphire (TGG crystal) from 30 *cm* (7 *cm*) to 110 *m* (28 *cm*) or more by adjusting the size of the input beam waist. Simple changes in the beam waist will enormously reduce thermal lensing.

Figure 3(b) shows the focal length variations due to the physical dimensions of the optics for a high absorption material such as Ti:sapphire ($P = 10W$ and $\omega_0 = 1mm$). A smaller longitudinal length and larger radial dimension result in a large focal length corresponding to a less thermal effect. It is evident that a larger radial dimension of optics makes the temperature distribution broader along the radial direction because our boundary condition requires constant temperature at $r = a$ and as a result, larger effective focal length is obtained. As the longitudinal length (l) increases, more energy from the input laser is absorbed and, consequently, the focal length from the thermal load will decrease. With further increase of the longitudinal length of the optics beyond the inverse of the absorption coefficients, most of the laser energy would be absorbed and hence the focal length will be saturated, as shown in Fig. 3(b). Figures 3(c) and 3(d) illustrate three-dimensional plots of variation in focal length with r and z for Ti:sapphire (c) and also a transparent optics as for TGG ($\omega_0 = 1mm$,

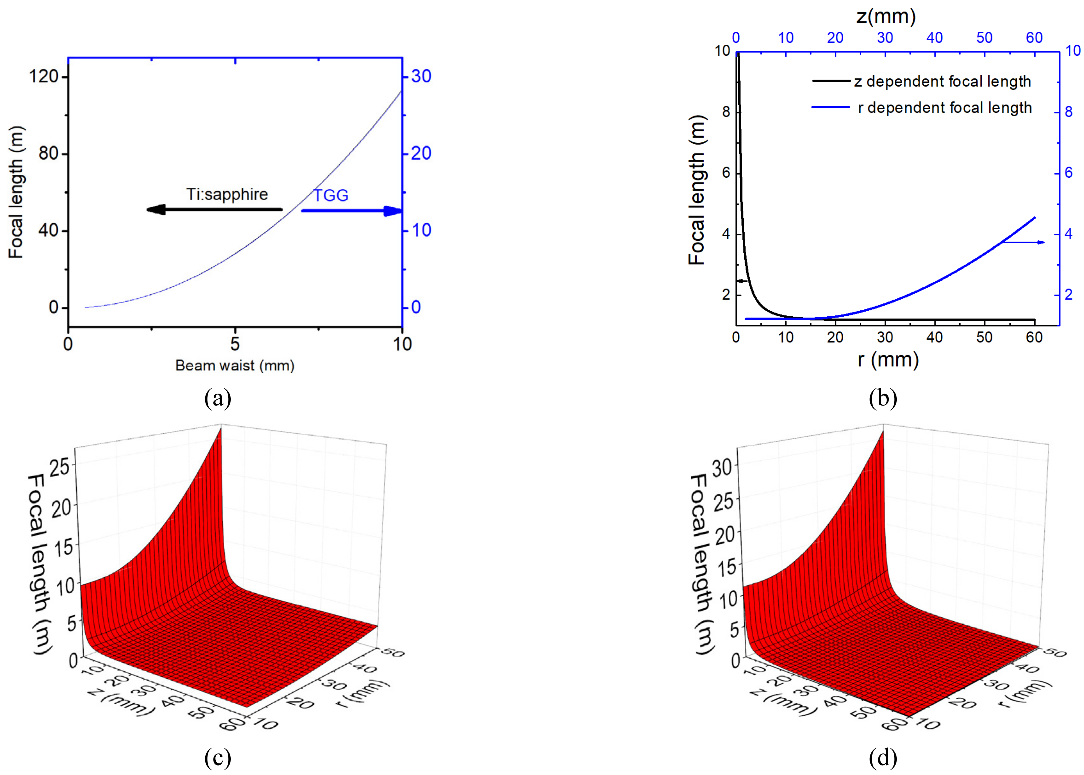

FIG. 3. (a) The focal length changes with beam waist for Ti:sapphire and TGG. All material parameters are the same as in Fig. 2 except for the beam waist. (b) Focal length changes depending on r (blue) with z = 10 *mm* and z (black) with r = 20 *mm* for Ti:sapphire with fixed beam waist of 1 *mm*. 3D plots of variation in focal length with geometry and z for (c) Ti:sapphire and (d) TGG.

$n = 1.954$, $\frac{dn}{dT} = 20\times10^{-6}/K$, $\alpha_{expansion} = 9.4\times10^{-6}/K$, and $P = 1KW$). Both cases demonstrate similar dimensional dependence of variation in focal length.

The above consideration of variation in focal length arising from thermal load induced by the laser should be the same in all optics as long as the boundary condition is the same as in Eq. (3).

Therefore, to reduce thermal lensing, larger beam waist and radial dimension of the optics and smaller laser power and longitudinal length of the optics are desired.

IV. CONCLUSION

To summarize, Eq. (16) could be essential to design a high power optic system, because if we know the total beam path in the system and material parameters, we could determine the focal length change of each optics and help to design compensating devices (In fact, we could make the total beam path of the system shorter than the focal length induced by thermal lensing to avoid unexpected damage of other optics). A technique to account for the induced thermal lensing is to introduce an additional lens to compensate and change the mode of the beam back to what it should be without thermal lensing, insert an active device designed to cancel out the thermal lensing [27], or place a suitable material having negative *dn*/*dT* immediately after the thermal lens to self-balance it [26]. In any case, an explicit analysis of the thermal effect on the material is a prerequisite before constructing these kinds of devices. It should be noted that our present analysis is restricted to the case of isotropic media and moderate temperature region. For the case of inhomogeneous media such as $GdVO_4$, YVO_4, etc., the heat flux q is represented in a more complicated form as follows

$$q_i = \Sigma_{i=1,2,3} \frac{\partial T}{\partial x_i} \tag{19}$$

because thermal conductivity is a tensor (different along different directions) [28, 29]. In these materials, both thermal conductivity and temperature derivative of refractive index are not only anisotropic but also temperature dependent [28] and coupled temperature equations should be solved [28, 30].

As a final remark, it would be also interesting to study the thermal effect of a double pump scheme in a laser cavity (laser pumping from both sides of the laser rod in a laser resonator [31]). In this case, the source term in Eq. (1) can be represented as $-\frac{2\alpha P}{\pi\omega^2} e^{-2\frac{r^2}{\omega^2}} (e^{-\alpha z} + e^{-\alpha(l-z)})$ and we easily obtain the temperature profile for the double pump scheme using Eq. (5). Because we need to integrate Eq. (13) along the z direction to investigate the thermal load from the laser, the focal length of the double pump scheme is the same as that of the single pump scheme as long as the total power of the laser remains the same.

In summary, we present the conditions to investigate thermal load from a Gaussian laser. This method is quite general and could be applicable to both transmissive and high absorptive optics. This result can be directly applied for the evaluation of thermal effects in the future development of high power laser technologies.

ACKNOWLEDGMENT

This research was supported by Basic Science Research Program through the National Research Foundation of Korea (NRF) funded by the Ministry of Education (2016R1D1A1 B03931391).

REFERENCES

1. J. D. Mansell, J. Hennawi, E. K. Gustafson, M. M. Fejer, R. L. Byer, D. Clubley, S. Yoshida, and D. H. Reitze, "Evaluating the effect of transmissive optic thermal lensing on laser beam quality with a Shack-Hartmann wave-front sensor," Appl. Opt. **40**, 366 (2001).
2. V. Quetschke, J. Gleason, M. Rakhmanov, J. Lee, L. Zhang, K. Y. Franzen, C. Leidel, G. Mueller, R. Amin, D. B. Tanner, and D. H. Reitze, "Adaptive control of laser modal properties," Opt. Lett. **31**, 217 (2006).
3. Z. Liu, P. Fulda, M. A. Arain, L. Williams, G. Mueller, D. B. Tanner, and D. H. Reitze, "Feedback control of optical beam spatial profiles using thermal lensing," App. Opt. **52**, 6452 (2013).
4. W. Koechner, *Solid-state laser engineering* (Springer-Verlag, 1998), Chapter 7.
5. V. Ramanathan, J. Lee, S. Xu, X. Wang, and D. H Reitze, "Analysis of thermal aberrations in a high average power single-stage Ti: sapphire regenerative chirped pulse amplifier: Simulation and experiment," Rev. Sci. Instrum. **77**, 103103 (2006).
6. B. Neuenschwander, R. Weber, and H. P. Weber, "Determination of the thermal lens in solid-state lasers with stable cavities," IEEE J. Quantum Electron. **31**, 1082 (1995).
7. G. Wagner, M. Shiler, and V. Wulfmeyer, "Simulations of thermal lensing of a Ti:Sapphire crystal end-pumped with high average power," Opt. Express **13**, 8045 (2005).
8. G. Mueller, R. S. Amin, D. Guagliardo, D. McFeron, R. Lundock, D. H. Reitze, and D. B. Tanner, "Method for compensation of thermally induced modal distortions in the input optical components of gravitational wave interferometers," Classical Quantum Gravity **19**, 1793 (2002).
9. M. Adier, F. Aguilar, and T. Akutsu et al., "Progress and challenges in advanced ground-based gravitational-wave detectors." Gen. Relativ. Gravitation **46**, 1749 (2014).
10. E. Wyss, M. Roth, T. Graf, and H. P. Weber, "Thermooptical compensation methods for high-power lasers," IEEE J. Quantum Electron. **38**, 1620 (2002).
11. M. A. Arain, V. Quetschke, J. Gleason, L. F. Williams, M. Rakhmanov, J. Lee, R. J. Cruz, G. Mueller, D. B. Tanner, and D. H. Reitze, "Adaptive beam shaping by controlled thermal lensing in optical elements," Appl. Opt. **46**, 2153 (2007).
12. R. Lawrence, D. Ottaway, M. Zucker, and P. Fritschel, "Active correction of thermal lensing through external radiative thermal actuation," Opt. Lett. **22**, 2635 (2004).
13. S. Sato, "Liquid-crystal lens-cell with variable focal length," Jpn. J. Appl. Phys. **18**, 1679 (1979).
14. J. Schwarz, M. Geissel, P. Rambo, J. Porter, D. Headley, and M. Ramsey, "Development of a variable focal length concave mirror for on-shot thermal lens correction in rod amplifiers," Opt. Express **14**, 10957 (2006).
15. K. Dobek, M. Baranowski, J. Karolczak, D. Komar, K. Kreczmer, and J. Szuniewicz, "Thermal lens in a liquid sample with focal length controllable by bulk temperature," Appl. Phys. B **122**, 151 (2016).
16. T. A. Meyers, *Encyclopedia of analytical chemistry* (John Wiley & Sons Ltd 2010).
17. J. Moreau and V. Loriette, "Confocal thermal-lens microscope," Opt. Lett. **29**, 1488 (2004).
18. W. Koechner, "Thermal lensing in a Nd:YAG laser rod," Appl. Opt. **9**, 2548 (1970).
19. U. O. Farrukh, A. M. Buoncristiani, and C. E. Byvik, "An analysis of the temperature distribution in finite solid-state laser rods," IEEE J. Quantum Electron. **24**, 2253 (1998).
20. M. Innocenzi, H. Yura, C. Fincher, and R. Fields, "Thermal modeling of continuous-wave end-pumped solid-state lasers," Appl. Phys. Lett. **56**, 1831 (1990).
21. A. Cousins, "Temperature and thermal stress scaling in finite-length end-pumped laser rods," IEEE J. Quantum Electron. **28**, 1057 (1992).
22. M. Schmid, T. Graf, and H. P. Weber, "Analytical model of the temperature distribution and the thermally induced birefringence in laser rods with cylindrically symmetric heating," J. Opt. Soc. Am. B **17**, 1398 (2000).
23. H. S. Carslaw and J. C. Jaeger, *Conduction of heat in solids* (Oxford Univ. 1948).
24. J. Lee, and D. H. Reitze, "Analytic spatial and temporal temperature profile in a finite laser rod with input laser pulses," Opt. Express **23**, 2591 (2015).
25. F. Kreitha and M. S. Bohn, *Principle of heat transfer*, 6th ed. (Brooks/Cole, CA, USA, 2001).
26. G. P. Kwon and J. Lee, "Self-adaptive thermal-lensing compensation for a high-power laser," J. Korean Phys. Soc. **69**, 1531 (2016).
27. R. Lausten, and P. Balling, "Thermal lensing in pulsed laser amplifiers: an analytical model," J. Opt. Soc. Am. B **20**, 1479 (2003).
28. A. H. Farhadian, H. Saghaffier, and M. Dehghanbaghi, "Calculation of thermal lensing in end-pumped YVO_4/Nd:YVO_4 composite crystals in view of the temperature distribution," J. Russ Laser Res. **36**, 350 (2015).
29. M. N. Ozisik, *Boundary value problems of heat conduction* (Dover Publications, INC 1968), pp. 457.
30. M. Sameti and A. Kasaeian, "Heat diffusion in an anisotropic medium with central heat source," Int. J. Partial Differ. Equations Appl. **2**, 23 (2014).
31. S. Ito, H. Nagaoka, T. Kobayashi, A. Endo and K. Torizuka, "Measurement of thermal lensing in a power amplifier of a terawatt Ti:sapphire laser," Appl. Phys. B **74**, 343 (2002).